Effect of electrode thickness variation on operation of capacitive deionization

Porada, S., Bryjak, M., Van der Wal, A., & Biesheuvel, P.M.

This is a "Post-Print" accepted manuscript, which has been published in "Electrochimica Acta".

Please cite this publication as follows:

Porada, S., Bryjak, M., Van der Wal, A., & Biesheuvel, P.M. (2012). Effect of electrode thickness variation on operation of capacitive deionization. Electrochimica Acta, 75, 148–156.

You can download the published version at:
http://dx.doi.org/10.1016/j.electacta.2012.04.083

Effect of electrode thickness variation on operation of Capacitive Deionization

S. Porada,[1,2,*] M. Bryjak,[2] A. van der Wal,[3,4] and P.M. Biesheuvel[1,4]

[1]*Wetsus, centre of excellence for sustainable water technology, Agora 1, 8934 CJ Leeuwarden, The Netherlands.* [2]*Department of Polymers and Carbon Materials, Faculty of Chemistry, Wroclaw University of Technology, Wybrzeze Wyspianskiego 27, 50-370 Wroclaw, Poland.* [3]*Voltea B.V., Wasbeekerlaan 24, 2171 AE Sassenheim, The Netherlands.* [4]*Department of Environmental Technology, Wageningen University, Bornse Weilanden 9, 6708 WG Wageningen, The Netherlands. e-mail: slawomir.porada@wetsus.nl.*

Abstract

In capacitive deionization (CDI) water is desalinated by applying an electrical field between two porous electrodes placed on either side of a spacer channel that transports the aqueous solution. In this work we investigate the equilibrium salt adsorption and the dynamic development of the effluent salt concentration in time, both as function of spacer and electrode thicknesses. The electrode thickness will be varied in a symmetric manner (doubling both electrodes) and in an asymmetric manner, by doubling and tripling one electrode but not the other. To describe the structure of the electrostatic double layer (EDL) which determines the salt adsorption in the micropores of activated carbons, a modified Donnan-model is set up which successfully describes the data, also for situations of very significant electrode thickness ratios. We develop a generalized CDI transport model accounting for thickness variations, which compares favorably with experimental data for the change of the effluent salt concentration in time. These experiments are aimed at further testing our equilibrium and transport models, specifically the assumption therein that in first approximation, for electrodes made of chemically unmodified activated carbon particles, the EDL structure is independent of the sign of the electronic charge. To investigate the effect of chemical surface charge we also varied the pH of the salt solution.

1. Introduction

Technologies where ions are removed from water by electrical fields include electro-deionization and electrodialysis [1, 2], water desalination using microchannels [3] and batteries [4], capacitive deionization (CDI) [5-30], and membrane capacitive deionization [31-36]. Recently a new promising application with focus on generating energy from mixing fresh and salt water has been demonstrated, which makes use of a capacitive flow process similar to that employed in CDI [37, 38]. In this manuscript we discuss capacitive deionization (CDI). CDI is a novel water desalination technology with the potential to desalinate water sources of various origins (ground water, industrial water, water for consumer applications) in an energy-efficient manner. The reason of low energy consumption is that CDI removes the relatively few salt ions from the salt-water mixture, instead of removing the majority component, which is the water, as is done in reverse osmosis and distillation.

How does CDI work? Briefly, in CDI an electrical potential difference is applied between two oppositely placed porous carbon electrodes. This is the cell voltage, V_{cell}. Because of the cell voltage, ions from the transport channel in between the electrodes are being removed and are stored inside the pores within the electrode, where electrostatic double layers (EDL) are formed, with cations stored in the cathode and anions in the anode. In this way partially desalinated water is produced. In the following step, the ions that are adsorbed in the electrode are released back into the transport channel by discharging the electrodes. As a result, a concentrated waste stream (brine) is produced. This cycle

consisting of the salt adsorption step and the salt release step can be repeated a very large number of times, with typical durations for each period of a few minutes. Note that the discussion that follows is based on this set-up, as just explained, i.e., a functional CDI cell with two porous (carbon) electrodes placed opposite one another, see Fig. 1, and not based on an electrochemical (three-electrode) experiment meant to characterize electrodes, where often only the working electrode is made of porous carbon.

In the CDI literature various conceptual approaches are used to describe operation of the electrodes in a CDI cell. One approach to describe CDI-performance stresses the importance that each electrode's potential is positioned appropriately relative to a reference potential or within a voltage window, to have optimized ion adsorption [7, 26, 27]. Based on this conceptual approach, it has also been argued that placing reference electrodes in the flow system can improve the salt adsorption capacity of the CDI-cell [26]. In another approach, reference potentials or voltage windows are not considered, but the focus is on how much charge is transferred from one electrode to the other, and how this impacts ion concentrations inside the porous electrodes and the resulting local voltage drops across the EDL. In this approach, classical EDL theory for capacitive, ideally-polarizable, electrodes can be used to describe the charge-voltage and salt-voltage characteristics of the cell. This is the approach taken in the present work.

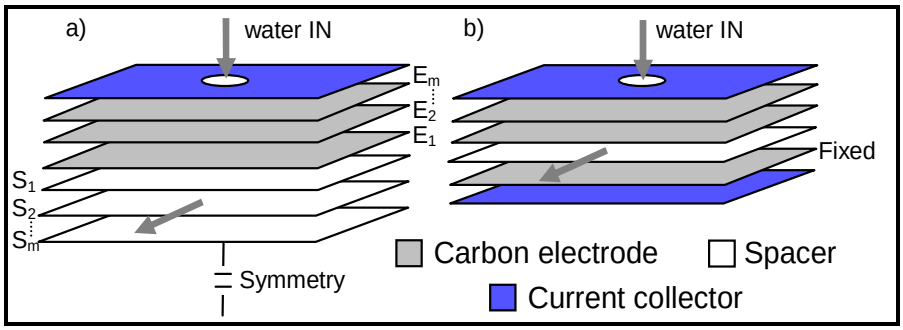

Fig. 1. Schematic representation of a Capacitive Deionization cell, with the possibility of a) Varying the thickness of spacer (S) and electrode (E) in a symmetric way, and b) Varying the cathode:anode mass ratio (mC:mA).

In this approach, when the electrodes do not carry chemical charge, and when we have an ideal 1:1 salt solution, then the important assumption of "similarity" can be made, which implies that the structure of the EDL does not depend on the sign of charge, with only the role of cations and anions reversed. This had the important consequence that when equal amounts of each electrode are used, and when we do not inject extra charge into the electrode pair, e.g., by an auxiliary capacitor or (reference) electrode, that then the total applied cell voltage can be equally divided over each of the two electrodes. Of course, even for those assumptions, similarity will never be exactly fulfilled, but as we will show it results in an excellent first order approximation of the behavior of a simple two-electrode CDI-system based on electrodes synthesized from chemically unmodified activated carbon powders. We will show that this approach works for symmetric cells, where the cathode mass is equal to the anode mass, but can also be applied to systems where the cathode mass is different from the anode mass. According to this approach, CDI is characterized by a certain transfer of charge from one electrode to the other, and an accompanying salt adsorption determined by the structure of the EDL in

the two electrodes. When equilibrium is reached, the various contributions to the potential of the EDL of the two electrodes combined (Stern layer, diffuse layer), sum up to the applied cell voltage.

To investigate the hypothesis of similarity in CDI operation, we have performed experiments with two-electrode CDI cells where we change the ratio of mass (thickness) of cathode relative to anode, and do so in both directions: we perform experiments with much increased cathode mass, and likewise with increased anode mass. The experiments are based on applying a cell voltage between the two oppositely placed porous electrodes, which are identical in composition, i.e., made of the same electrode material. We do not use reference electrodes. If the assumption of similarity is valid, then the experiment with three times more cathode material should basically give the same performance (salt adsorption, and charge stored) as the experiment with three times more anode. These are novel experiments, because up to now CDI desalination experiments using cells with two porous electrodes have always used electrodes of equal mass (thickness). We also use these experiments to validate and check our existing theoretical models, both for the modified Donnan model [29, 35, 39] which describes the equilibrium cell performance, and for the full CDI cell dynamic transport model [35]. To validate those models further we also vary the spacer thickness and absolute amount of electrodes (i.e., by doubling both electrodes). In this way information is obtained on the relative importance of the resistance for ion transport in spacer and in electrode. These various geometrical options are summarized in Fig. 1.

A second important and related discussion in the CDI-literature is the possible role of chemical effects, such as pseudo-capacitance, oxygen reduction, and chemical surface charge, with chemical charge related to the point of zero charge of the carbon [23, 25, 27]. Of course, these chemical phenomena are well-known to exist in carbon electrodes and must also play a role in CDI. However, it is an open question how much influence these effects actually have on salt adsorption in CDI. As a first approximation, can such effects perhaps be neglected when describing CDI performance? Of the various effects, here we only address the role of chemical surface charge, e.g. due to acidic or phenolic groups in the carbon particles. If this chemical charge is important, then one expects that desalination performance depends on pH, because pH influences the ionization degree of such surface groups [40, 41]. For instance, acidic groups reduce their charge at lower pH (are increasingly protonated, thus neutralized at low pH). To investigate this question, we performed experiments in which the inflow pH was varied between pH 4 and 10 and we checked the equilibrium charge and salt adsorption, both for a symmetric CDI cell (equal thickness of both electrodes) and for asymmetric systems. This is the first paper to report the effect of inflow pH on two-electrode CDI cells (previous work reported effluent pH changes in time [23]).

2. Experimental

Experimental details of the CDI stack (by stack we mean the assembly of a number N=8 of parallel cells) have been outlined before [22, 29, 35] and will briefly be summarized here. Materials used are graphite current collectors (thickness δ=250 μm), electrodes made of activated porous carbon particles (Materials & Methods, PACMM^{TM} 203, Irvine, CA, USA, δ_e=250 μm, mass of a single electrode 0.49 g), and a polymer spacer (Glass fibre prefilter, Millipore, Ireland, compressed thickness of a single layer,

δ_{sp}=250 μm). One CDI cell consists of one spacer, two electrodes, and two current collectors. We vary the electrode thickness by placing several electrodes on top of each other, see Fig. 1. In some experiments we also use two spacer layers on top of each other.

Each current collector is used for two adjacent cells (except for the two outer ones in the stack), and is used to inject electrons into both porous electrodes with which it is in direct contact (one on each side). These two electrodes will have the same polarity (either anode or cathode). Thus in the stack, the sequence of anode/cathode is reversed from cell to cell. After assembly, all layers in the stack are compressed and placed in a transparent housing. The stack is fed from a 10 liter vessel storing a NaCl-solution as the electrolyte of which the pH is stabilized by a pH controller (Liquisys-M, Endress+Hauser GmbH, Switzerland), and to which the effluent is recycled. We bubble N_2 through the storage vessel to keep oxygen out of the system. The salt solution is pumped into an inner square hole (1.5x1.5 cm^2) located in the middle of each cell and flows radially outward through the square 6x6 cm^2 spacer channel and leaves the spacer layer on all four sides. The conductivity of the effluent is measured on-line and is converted into salt concentration according to a calibration curve. We also measure effluent pH and correct the measured conductivity for pH-effects.

Note that in our experiments we measure the conductivity of the water in the effluent leaving the stack, and not in our large recycle vessel. Thus, after applying a non-zero cell voltage, the measured effluent conductivity will start to decrease, because of the desalination of the water flowing through the CDI stack. In time, the electrodes become saturated, and the applied cell voltage drops off in the EDLs within the electrodes, and there no longer remains a driving force for ions to be transported from the spacer channel into the electrodes. Consequently, the salinity of the effluent water increases again, up to the value of the inlet salt solution, see Figs. 6 and 7. When this final situation is reached, the water entering the CDI stack will no longer be desalinated, and leaves the stack unchanged. Thus, in this procedure the measured effluent conductivity first decreases in time and then increases again, back to the value of the inlet conductivity. In the next phase of the cycle, upon reducing the voltage to a lower value (e.g. to V_{cell}=0 V, which starts the ion desorption step), the ions are released again from the electrodes, and temporarily we observe a peak in effluent concentration, see e.g. Fig. 3 in ref. [22] and Fig. 2 in ref. [23]. This approach is different from the measurement of the conductivity in a (relatively small) recycle beaker, from which the stack is fed and to which the effluent is returned. Measuring conductivity there, one observes the conductivity to steadily decline during desalination, and to steadily increase again during ion release, see for instance refs. [14, 21, 32], without observing the distinct minima/maxima that we find in our procedure. The advantage of our approach is that when equilibrium is reached, the system has become equilibrated with a solution of a-priori set salt concentration, and thus it is possible to do sets of experiments with varying cell voltage and electrode mass, all in equilibrium with water of the same salt concentration. And this makes it possible to compare many data sets simultaneously with the same theoretical model, as we do below in Figs. 3-5.

In our experiments, the cell voltage is applied using a power supply (ES 030-5, Delta Elektronika B.V., Netherlands) and the current is measured simultaneously by a multimeter (Fluke 8846A, Fluke Corp., USA). A CDI-cycle consists of applying a positive constant cell voltage between anode and cathode during the salt adsorption step (salt removal step) of a duration of 1 hour, while in the reverse

step the cell voltage is set to zero and the adsorbed salt is released again (also for a duration of 1 hour). This cycle is repeated a few times before measurements are taken. The salt adsorption and charge in a CDI-cycle can be derived from the data of effluent salt concentration vs time, and of electric current vs time, by the following procedure. For salt adsorption, the difference between inflow salt concentration and outflow salt concentration is integrated with time, and multiplied with the water flow rate, while for charge the current is integrated with time. Except for the first one or two cycles, the measured salt adsorption upon applying the cell voltage is close to the salt release after reducing the voltage to zero, i.e., salt balance is maintained. Likewise, the integrated charging current is close to the integrated discharging current, and we have charge balance in a cycle.

3. Theory

In this section we describe the modified Donnan model for CDI systems with different amounts of anode relative to cathode. This was not done in previous models where both electrodes were assumed to have the same mass, and thus symmetry was assumed and only one half of the cell was considered. After that, the transport model of ref. [35] will be extended to include different electrode thicknesses. We describe an aqueous solution consisting of a fully dissociated monovalent salt. The transport model assumes that across the spacer (from electrode to electrode) concentration gradients are small. However, in the direction of flow, concentration changes are considered.

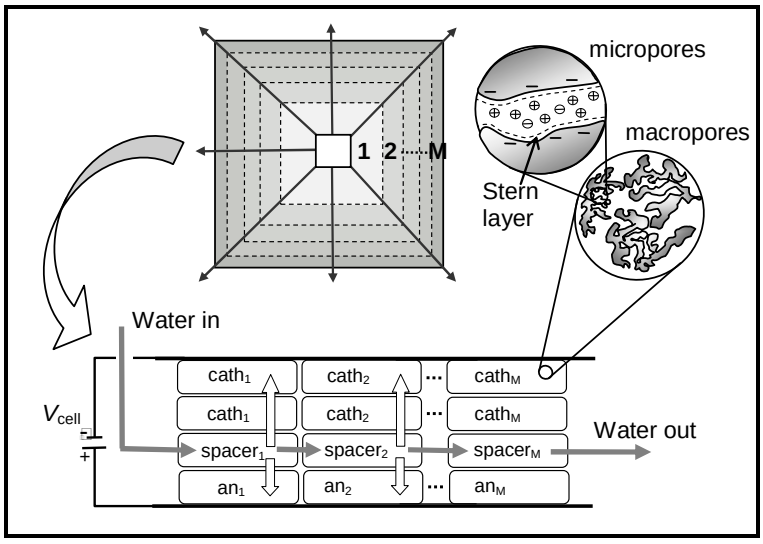

Fig. 2. Top view of CDI cell, and its description by a set of sequential sub-cells, including the possibility of unequal masses of anode and cathode. Within the electrode, the modified Donnan model describes the structure of the electrostatic double layer formed in the micropores inside the carbon particles.

3.1 Electrostatic double layers in porous electrodes – modified Donnan model

Within the electrodes, the open space (filled by electrolyte) is assumed to consists of two types of porosity, namely macropores and micropores. This is a simplified approach and more formal approaches are available [42]. Macropores with porosity p_{mA} form the open space *in between* the carbon particles and are responsible for transporting the ions across the electrode. Micropores with porosity p_{mi} are the nm-sized pores *within* the carbon particles, where the EDLs are formed and counterions are preferentially stored. Both porosities p are defined per total volume of the electrode. In

the macropores, we assume that $c_{cation,mA}$ has the same concentration as $c_{anion,mA}$ (=c_{mA}, defined per unit of macropore volume). In the present model for CDI, this concentration is the same as in the spacer channel, an assumption which can be relaxed when using a full porous electrode transport model [39, 43]. Instead, in the micropores the cation concentration, $c_{cation,mi}$, will differ from the anion concentration, $c_{anion,mi}$ (ion concentration per unit of micropore volume), with the difference being equal to the micropore ionic charge, $c_{charge,mi}$, which is compensated by an equal but opposite electrical charge in the electron-conducting carbon matrix. Because the size of the micropores is much smaller than that of the Debye length (a length scale to characterize the thickness of the diffuse part of the double layer in the classical Gouy-Chapman-Stern theory for a single double layer), the EDLs within the micropores will overlap strongly, resulting in an almost unvarying potential and ion concentration across the pore radius. Assuming the electrostatic potential and concentration in the micropore space to be constant across the pore radius, is the Donnan approach. The potential drop from outside the micropore (i.e., in the macropores) to inside, is the Donnan potential, $\Delta\phi_d$. (All parameters $\Delta\phi$ in this work are dimensionless voltage differences, and can be multiplied by the thermal voltage $V_T=RT/F$~25.7 mV at room temperature, to obtain a dimensional voltage). Taking this Donnan approach, the micropore concentration is related to that in the macropores according to

$$c_{j,mi} = c_{mA} \cdot \exp\left(-z_j \cdot \Delta\phi_d + \mu_{att}\right) \tag{1}$$

where z_j=+1 for the cation and z_j=-1 for the anion, and μ_{att} is an attractive term, describing a non-electrostatic driving force for ions to be inside the carbon micropores, relative to outside [44]. In the present work we will use the same value of μ_{att} for both the cation (Na^+) and the anion (Cl^-), though in a generalized model this assumption can be relaxed.

The difference between $c_{cation,mi}$ and $c_{anion,mi}$ is defined as the 'charge concentration', $c_{charge,mi}=c_{cation,mi}-c_{anion,mi}$ in the micropores. This charge, $c_{charge,mi}$, can be of both negative and positive sign (typically being negative in the anode, and positive in the cathode) and is locally charge-compensated by an equal but opposite electronic charge in the carbon matrix. The charge concentration, $c_{charge,mi}$, relates to the potential difference across a nanoscopic Stern layer, $\Delta\phi_{St}$, envisioned to be located in between the water-filled micropores and the carbon matrix, according to

$$c_{charge,mi} \cdot F = -V_T \cdot \Delta\phi_{St} \cdot C_{St,vol} \tag{2}$$

where F is the Faraday constant (96485 C/mol) and $C_{st,vol}$ is a volumetric capacitance of the Stern layer. As is explained in refs. [29, 35], we use for the Stern capacity, $C_{St,vol}$, the empirical expression $C_{St,vol}=C_{St,vol,0}+\alpha\cdot(\Delta\phi_{st})^2$ making the Stern capacity increase slightly with Stern layer voltage. This modification gives a better fit of the theory to the data, and can be rationalized as being due to larger forces across the dielectric Stern layer at high Stern voltage (proportional with charge), resulting in the ions approaching the carbon surface more closely, a thinner Stern layer as result, and thus an increase in its capacity [45, 46].

The above paragraphs explain the modified-Donnan (mD) model for a single electrode. How to describe a set of two electrodes between which a cell voltage of V_{cell} is applied? First of all, at equilibrium (i.e., the process of ion adsorption has come to an end) the cell voltage is built off in the two EDLs, both of which have a contribution from the Donnan potential, $\Delta\phi_d$, and Stern potential, $\Delta\phi_{St}$, thus

$$V_{\text{cell}}/V_{\text{T}} = \left(\Delta\phi_{\text{d}} + \Delta\phi_{\text{St}}\right)_{\text{micropores,anode}} - \left(\Delta\phi_{\text{d}} + \Delta\phi_{\text{St}}\right)_{\text{micropores,cathode}}. \quad (3)$$

Next we can define the mass difference mCmA, the ratio of the mass of cathode to anode. A charge balance can be set up according to

$$c_{\text{charge,mi}}\big|_{\text{cathode}} \cdot \text{mCmA} = -c_{\text{charge,mi}}\big|_{\text{anode}} \quad (4)$$

which is consistent with the fact that each electron taken away from the anode will go to the cathode. Note that Eq. 4 can only be used when the charge is assumed to be homogeneously distributed across the electrode, and gradients in $c_{\text{charge,mi}}$ through the electrode can therefore be neglected.

This set of equations describes ion concentrations in the micropores at equilibrium, when ion transport has stopped and thus the concentration in the macropores, c_{mA}, will be equal to the salt concentration flowing into the cell, $c_{\text{salt,in}}$. To convert to the measurable properties of charge transferred Σ (in mol/g; multiply by F to obtain charge Σ_F in C/g) and salt adsorbed Γ_{salt} (also in mol/g; both Σ and Γ_{salt} are defined per gram of total electrode mass) as plotted in Figs. 3, 4 and 5, we must first of all define a total micropore ion concentration as $c_{\text{total ions,mi}} = c_{\text{cation,mi}} + c_{\text{anion,mi}}$, secondly emphasize that at V_{cell}=0 V already some salt is adsorbed in the micropores due to the chemical attraction, even though at V_{cell}=0 V the micropore charge is zero, and thirdly note that in the experiment we measure the difference in salt adsorption between that at a non-zero cell voltage and that at the value of V_{cell}=0 V. It is a difference in salt adsorption that we measure because prior to applying the nonzero cell voltage, we equilibrate the cell for a long time with the aqueous solution, while the two electrodes are short-circuited and thus V_{cell}=0 V during that period. The conversions from $c_{\text{charge,mi}}$ and $c_{\text{total ions,mi}}$ to equilibrium charge Σ and salt adsorption Γ_{salt} (relative to the salt adsorption at zero applied voltage, i.e., at V_{cell}=0 V) are given by

$$\Gamma_{\text{salt}} = \frac{p_{\text{mi}}}{2\rho_{\text{e}}\left(\text{mCmA}+1\right)} \cdot \left[\text{mCmA} \cdot \left(c_{\text{total ions,mi}} - c^{0}_{\text{total ions,mi}}\right)\big|_{\text{cathode}} + \left(c_{\text{total ions,mi}} - c^{0}_{\text{total ions,mi}}\right)\big|_{\text{anode}}\right] \quad (5)$$

and

$$\Sigma = \frac{p_{\text{mi}}}{\rho_{\text{e}}}\frac{\text{mCmA}}{\text{mCmA}+1} \cdot c_{\text{charge,mi}}\big|_{\text{cathode}} = -\frac{p_{\text{mi}}}{\rho_{\text{e}}}\frac{1}{\text{mCmA}+1} \cdot c_{\text{charge,mi}}\big|_{\text{anode}} \quad (6)$$

where ρ_{e} is the electrode density and superscript "0" refers to the ions adsorption in the micropores at V_{cell}=0 V. Eqs. 5 and 6 reduce to similar equations (Eq. 13 in ref. [35]) when mCmA=1, i.e. when we have equal amounts of both electrodes. From the above equations we can derive the charge efficiency, Λ, which is the equilibrium ratio of salt adsorption Γ_{salt} over charge Σ, thus

$$\Lambda = \frac{\Gamma_{\text{salt}}}{\Sigma}. \quad (7)$$

Equilibrium calculation results in Figs. 3-5 to be discussed in the next section, are based on Eqs. 1-7 listed above.

3.2 Transport model for ion transport in spacer channel

The dynamic (time-dependent) behavior of the CDI-system is described by the transport model of ref. [35]. In the present work, the theory is extended to include the situation of unequal amounts of electrode. Therefore the symmetry assumption as made previously must be discarded, and each

electrode is described separately using Eqs. 1 and 2 above. Eq. 3 is extended to include a voltage drop, $\Delta\phi_{tr}$, due to a resistance which is a summation of a spacer resistance and an electrode resistance. We will not describe ion transport within the electrode in detail [39, 43], but take a simplified approach and empirically include an electrode resistance in which the electrode voltage drop depends on current and macropore ion concentration. Because in our CDI model (not in the models for MCDI as in ref. [35]) the macropore concentration is assumed to be equal to the spacer concentration, this extra voltage drop has a dependence on ion current and salt concentration that is of the same form as for the spacer channel. Thus we combine the electrode resistance with that in the spacer and replace Eq. 3 by

$$V_{cell}/V_T = \left(\Delta\phi_d + \Delta\phi_{St}\right)_{micropores,anode} + \Delta\phi_{tr} - \left(\Delta\phi_d + \Delta\phi_{St}\right)_{micropores,cathode}. \tag{8}$$

In this approach, the ion current density directed across the channel, from electrode to electrode, with dimension mol/(m^2.s), relates to $\Delta\phi_{tr}$ according to

$$I = 2D \cdot c_{salt,sp} \cdot \left(d \cdot \delta_{sp} + \delta_e^{eff}\right)^{-1} \cdot \Delta\phi_{tr} \tag{9}$$

where D is the average diffusion coefficient of anion and cation in free solution, and $c_{salt,sp}$ the spacer salt concentration which depends on time and the position in the flow direction, but is assumed to be constant in the direction from electrode to electrode, i.e., Eq. (9) assumes that there are no concentration gradients across the width of the channel. The two parameters d and δ_e^{eff} describe the relative contributions to the total resistance, of 1. the spacer, and 2. of both electrodes combined. The constant parameter d describes how the effective spacer thickness, to be used in Eq. 9, is a constant multiple of the geometric thickness, δ_{sp}, which in our experiments is δ_{sp}=250 μm for a single spacer experiment, and 500 μm for a double spacer. The ion current density I from the spacer channel into each of the electrodes relates to charge buildup in the electrodes according to

$$\delta_e \cdot \frac{\partial}{\partial t}\left(p_{mi} \cdot c_{charge,mi}\right) = \pm I \tag{10}$$

where δ_e is the electrode thickness. We define the current to be positive when it runs from anode to cathode, and thus the plus-sign in Eq. 10 is for the cathode, and the minus-sign for the anode.

The total ion flux entering an electrode, J_{ion}, relates to the ion accumulation according to

$$\delta_e \cdot \frac{\partial}{\partial t}\left(2 \cdot p_{mA} \cdot c_{mA} + p_{mi} \cdot \left(c_{cation,mi} + c_{anion,mi}\right)\right) = \pm J_{ion} \tag{11}$$

where c_{mA} is the salt concentration in the macropores, assumed to be equal to $c_{salt,sp}$. Note that the ion current I is the same for both electrodes (also when there is a thickness ratio), but this is not the case for J_{ion}, which will be different for the anode and the cathode.

It is important to note that the above set of equations is not solved only once for the entire cell in its entirety. Instead, to describe the ongoing desalination in the flow direction (from entrance to exit of the cell), we model the CDI cell as a set of subsequent “stirred volumes” or “sub-cells”, the number of which in the calculation will be M, see Fig. 1. In each sub-cell, the above set of equations 1-11 is solved, together with a salt mass balance for each spacer sub-cell, as given by

$$\delta_{sp} \frac{\partial c_{salt,sp}}{\partial t} = -\tfrac{1}{2}\left(J_{ions,cathode} - J_{ions,anode}\right) - \delta_{sp} \frac{M}{\tau_{sp}}\left(c_{salt,sp} - c_{salt,sp,IN}\right) \tag{12}$$

where on the left-hand side we have the accumulation of salt in the spacer sub-cell, and where on the right-hand side the first term is the ion transport from the channel into the electrodes, both at the anode and cathode sides (the factor ½ is because a salt flux is half a total ions flux) and the final term is the convective salt transport in the direction along the electrode from one sub-cell to the next. Here, $c_{salt,sp,IN}$ is the inlet salt concentration into the sub-cell, which for the very first sub-cell is equal to the feed concentration, $c_{salt,0}$, and otherwise is equal to $c_{salt,sp,i-1}$, i.e., equal to the effluent of the sub-cell prior to it in upstream direction.

In Eq. 12, τ_{sp} is the total spacer channel residence time (the spacer channel open volume, V_{sp}, divided by the spacer channel flow rate, Φ_{sp}). For V_{sp} we can take the geometric dimensions (thickness times electrode area), but we can also consider a volume reduction because of the presence of the polymer spacer material with a typical open volume of 50-80 vol%. In any case, for a twice-thicker spacer, the residence time will double. In the present work we neglect the residence time reduction because of the polymer spacer material. Thus, we model the system as if the channel is open, i.e., all volume is available for the aqueous solution.

Finally, the water leaving the last subcell is mixed up in the space surrounding the N cells (dead volume), before flowing through an exit tube along the conductivity meter which measures the effluent salt concentration, $c_{effluent}$, as plotted in Figs. 6 and 7. The effect of the dead volume is described as a stirred volume according to

$$V_{dead}\frac{\partial c_{effluent}}{\partial t} = N\Phi_{sp}\left(c_{salt,sp,M} - c_{effluent}\right). \tag{13}$$

The model as explained above predicts $c_{effluent}$ as function of time, cell voltage, water flow rate, inflow salt concentration, spacer thickness and electrode thickness (which can be different for anode and cathode), electrode macro- and microporosities, and as function of EDL properties such as μ_{att} and $C_{St,vol}$. The model outcome can be compared to the experimental observations, as we do in Figs. 6 and 7. All parameters which are used in our theoretical calculations are listed in Table 1.

ρ_e	electrode mass density	0.600	g/ml
δ_e	thickness of single electrode	242	μm
p_{mA}	porosity of macropores	30	%
p_{mi}	porosity of micropores	30	%
$C_{St,vol,0}$	volumetric Stern layer capacitance	120	MF/m^3
α	parameter to describe non-linear Stern capacity	0.10	MF/m^3
D	ion diffusion coefficient in the spacer channel	$1.68\cdot10^{-9}$	m^2/s
A	electrode area in one cell	33.8	cm^2
δ_{sp}	spacer thickness (single spacer)	250	μm
μ_{att}	chemical attraction term for ion to go into micropores	2.0	kT
Φ_{sp}	spacer channel flow rate	7.5	ml/min
V_{dead}	dead volume	75	ml
d	correction factor for resistance in spacer channel	6	
δ_e^{eff}	effective two-electrode thickness for resistance model	1000	μm
M	number of sub-cells in the model	6	

Table 1. Parameter settings for CDI transport model.

4. Results and Discussion

4.1 Effects of electrode thickness variation on CDI performance

In this section we discuss experimental and theoretical results of the maximum salt adsorption Γ_{salt} (equilibrium adsorption) and charge Σ_F (=$\Sigma \cdot F$, with Σ used in the Theory-section and defined in mol/g, with F Faraday's number) for the symmetric and asymmetric cell configurations, which implies different masses of cathode and anode used inside the CDI stack. Note that our standard way of defining salt adsorption and charge in this work is per mass of all electrodes combined, as we use in Figs. 3 and 5. This is also the definition used in Eqs. (5) and (6). In Fig. 4 we will use a different definition because it shows more clearly how much the salt adsorption and charge of a CDI-cell increase when we add one or more layers of electrode.

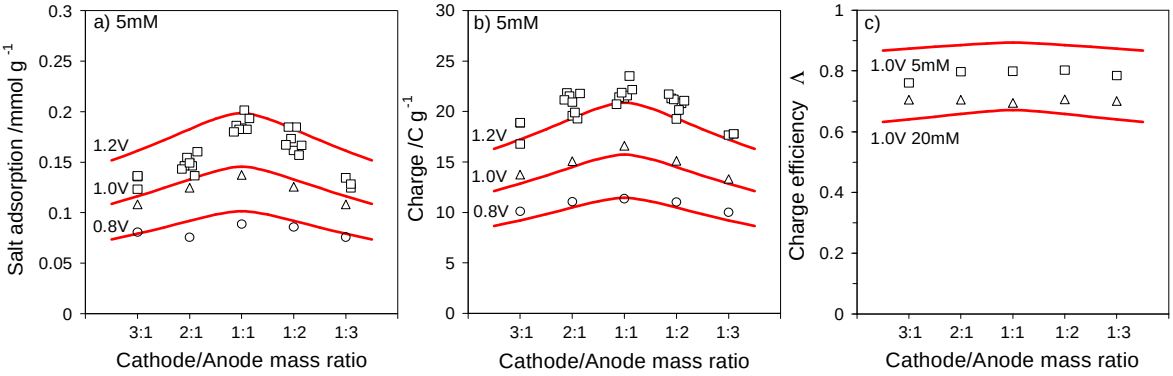

Fig. 3. (a,b) Equilibrium data for CDI cell performance per gram of all electrodes combined, as function of cathode:anode mass ratio (mC:mA) and cell voltage ($c_{salt,in}$=5 mM). (c) Charge efficiency, Λ, at two values of $c_{salt,in}$. Comparison with the modified Donnan (mD) model (lines

As Fig. 3 shows for $c_{salt,in}$=5 mM (background concentration of NaCl), the highest values of Γ_{salt} and Σ_F are found when equal amounts of both electrodes are used (mCmA=1). With an increasing mass ratio difference, we observe a gradual decrease of Γ_{salt} and Σ_F. Importantly, as Fig. 3 shows, we find that the decrease in Γ_{salt} and Σ_F with increasing mass asymmetry does not depend on whether we used an excess of anode, or an excess of cathode, i.e. the data are the same for mCmA=2 (or 3) as for mCmA=1/2 (or 1/3), except data for Γ_{salt} at 1.2 V for 5 mM at mCmA=0.5/2, which show a small difference between the two sets of experiments. These observations support the idea that for the electrodes and electrolyte that we use, the EDL-structure that develops in the micropores does not depend on the sign of the surface charge in the carbon matrix, i.e., the assumption of similarity seems to be valid. This would also imply that when we use mCmA=1, i.e., a symmetric cell, and when we are at equilibrium, and when we do not (pre-)charge the CDI-pair by a third electrode, that the applied cell voltage will be equally distributed between the two electrodes, and thus symmetry can be assumed. Thus, for the simple two-electrode system, it is the cell voltage, i.e., the voltage which can be applied between two porous electrodes, that fully determines salt adsorption and charge in CDI.

The charge efficiency, Λ, which is the ratio between the equilibrium salt adsorption, Γ_{salt}, and the stored charge, Σ, quantifies how many 1:1 salt molecules are adsorbed from solution for each electron transported from anode to cathode during the adsorption step, for the condition that equilibrium has

been reached in the cell, and salt and charge flow into the electrode have come to a stop. Charge efficiency is an important parameter determining salt removal performance and energy consumption in CDI. Fig. 3c shows data for Λ obtained from the equilibrium data for Γ_{salt} and Σ from Fig. 3a,b. What can be observed is that the experimental data reach a plateau value of Λ~0.8 for V_{cell}=1.0 V and $c_{salt,in}$=5 mM NaCl, which is in good agreement with our previous findings described in refs. [22, 29, 35].

Fig. 3c also shows that charge efficiency only slightly depends on the cathode/anode mass-ratio, mCmA. This would suggest that for optimal system performance we are relatively free to use quite asymmetric electrode pairs, without reducing the charge efficiency much, and thus without substantially affecting salt removal performance and energy demand. Of course the thickness of the electrodes cannot be increased infinitely, because for thick electrodes the ions will not penetrate the whole electrode structure anymore within a reasonable period of time.

In Fig. 4, data of Fig. 3a,b are plotted again, but now defined per mass of the "standard" system, which is one layer of cathode and one layer of anode (i.e., the case of mCmA=1). Thus these data show how the performance of a cell (stack) improves when we add extra layers of electrodes on only one side of the cell. Also data for $c_{salt,in}$=20 mM are presented. Interestingly, salt adsorption and charge significantly increase when we add extra layers of electrodes, despite the increasing asymmetry.

Instead, intuitively, one might perhaps think that when building an asymmetric cell, that the minority electrode will limit the overall capacity. However, the data show quite the opposite trend, namely that salt adsorption significantly increases when we add electrodes, even when this leads to a very asymmetric cell design. To explain this, one must consider that in such an asymmetric design the cell voltage distributes in such a way that the minority electrode has much higher charge density and salt adsorption density (i.e., per gram of electrode) than the other electrode. Because of this, the overall salt adsorption of the system (per total mass of all electrodes combined) apparently only weakly depends on an asymmetric mass distribution of the two electrodes (Fig 3a,b). Importantly, the modified Donnan model (lines in Fig. 3 and 4; described by Eqs. 1-7) very well reproduces the effect of mass asymmetry on salt and charge storage. Using a single set of parameter settings for $C_{St,vol,0}$, α, μ_{att} and the single group p_{mi}/ρ_e, values for which are given in Table 1, the model quite accurately describes the data, though data for salt adsorption for asymmetric systems are overestimated for 1.2 V/5 mM, and are underestimated for 1.0 V/0.8 V/20 mM.

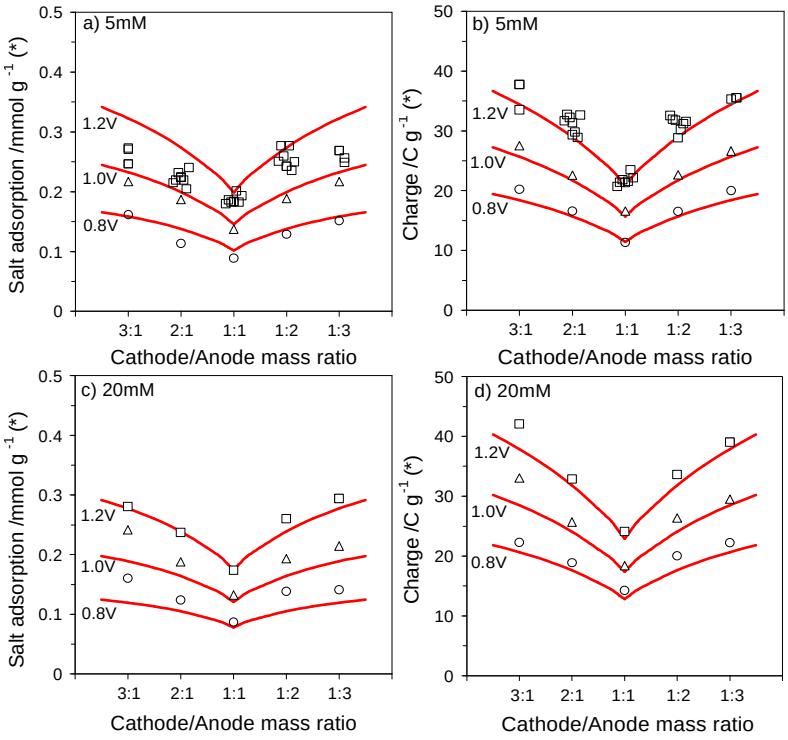

Fig. 4. Equilibrium data for CDI cell performance per gram of standard cell configuration, as function of cathode:anode mass ratio (mC:mA), salt concentration, and cell voltage. Comparison with modified Donnan (mD) model (lines). (a,c). Salt adsorption Γ_{salt} . (b,d). Charge, Σ_F.

4.2 Effects of pH on CDI equilibrium performance

In the next set of experiments we varied the pH of the inflowing solution, to study the effect of surface chemical charge on desalination. Our assumption is that the surface chemical charge will be sensitive to pH, and thus when chemical surface charge plays a role in salt adsorption, salt adsorption should depend on the pH of the feed solution. Results of our experiments are presented in Fig. 5. The data presented in Fig. 5 reveal only minor (or inconsistent) effects of feed pH on salt adsorption and charge. For the standard design (mCmA=1), and across the whole pH window tested, Γ_{salt} and Σ_F remain close to the value of 0.18 mmol/g and 22 C/g, respectively, without any clear dependence on pH. If chemical surface charge effects are important for CDI, it seems reasonable to assume that we should have seen a stronger and more consistent impact of the feed pH on salt adsorption and charge in CDI, but however this is not the case.

For asymmetric cells, we see that the charge transferred Σ_F is independent of pH. For salt removal Γ_{salt} we see much scatter, but we cannot discern a clear pattern in the influence of pH on Γ_{salt}. In summary, based on our experimental observations, as presented in Fig. 5, we conclude that chemical surface charge effects do not seem to influence salt adsorption and charge in a very notable fashion, at least not for the electrodes and electrolyte that we tested.

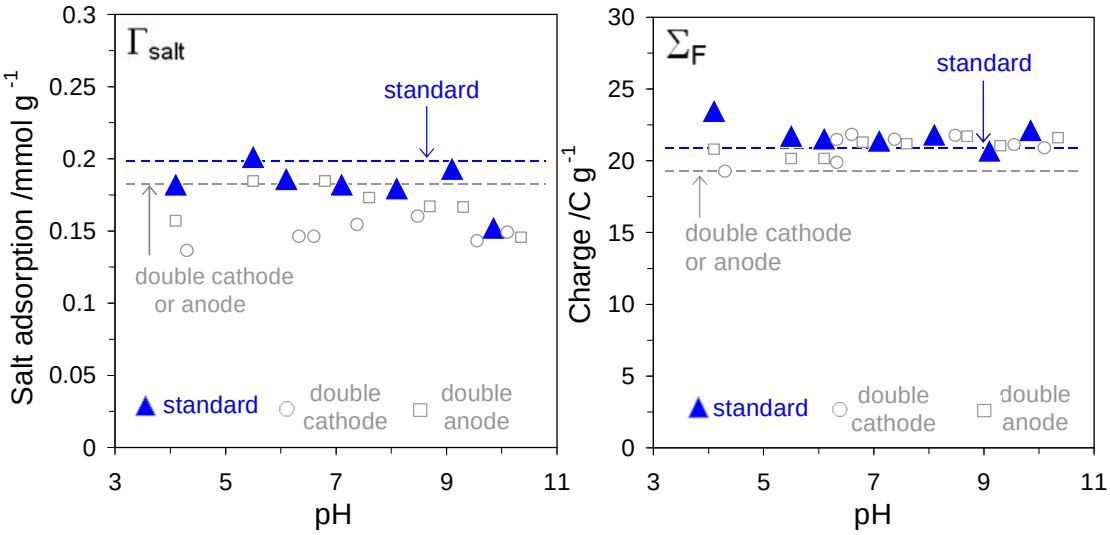

Fig. 5. Equilibrium salt adsorption Γ_{salt} and charge Σ_F as function of pH of the inflowing solution, for three cell configurations ($c_{salt,in}$=5 mM, V_{cell}=1.2 V). Lines based on modified Donnan (mD) model.

4.3 The dynamics of the CDI process

Finally, the extended CDI transport model is tested by comparison with experiments in which the spacer channel thickness, as well as the electrode thickness (ratio) is varied. Fig. 6 compares experimental and theoretical dynamic curves for three cell configurations, and at two values of the cell voltage, and a good fit of the theory to the data is observed. One question is how to include the spacer and electrode resistance in the dynamic CDI model. For the spacer, a doubling of thickness results in a doubling of spacer resistance. However, for the electrode the situation is different, because charge storage is distributed across the electrode. This implies that at early times only the outer layer of the electrode is active, and gradually in time more and more electrode material is used for ion storage. The correct description for the influence of electrode thickness on CDI performance requires porous electrode theory, see refs. [39, 43]. As a simplification, in the present work we assume no dependence of the total resistance on a variation in electrode thickness. With these approaches, we find that we can rather well describe the various curves using the values for d and δ_e^{eff} as given in Table 1. Finally, in Fig. 7 we use the same model for the asymmetric cell designs, and also here find a good agreement between data and theory.

Small differences observed between the dynamic curves for double cathode vs that for double anode (mCmA=2 vs. ½) and between triple cathode and triple anode (mCmA=3 vs. 1/3) [curves for double anode and triple anode not reported] may be due to the use of NaCl, where the cation Na^+, has a 30% lower diffusion coefficient, D, than of the anion, Cl^-. Such differences in D have no impact on the equilibrium EDL properties as reported in Figs. 3-5, but will influence the dynamics of the desalination process. If indeed the difference in D between anion and cation is the origin of differences in the dynamic curves for asymmetrically constructed cell pairs, then the use of KCl as salt (for which D for cation and anion is close to equal) should give almost identical dynamic curves for effluent concentration vs. time (and current vs. time) when we compare an experiment with mCmA=x vs. an experiment with mCmA=1/x. The outcome of such an experiment would shed further light on the

validity of the assumption of similarity of the EDL structure in CDI electrodes based on electrodes made of activated, but chemically unmodified, carbon powders.

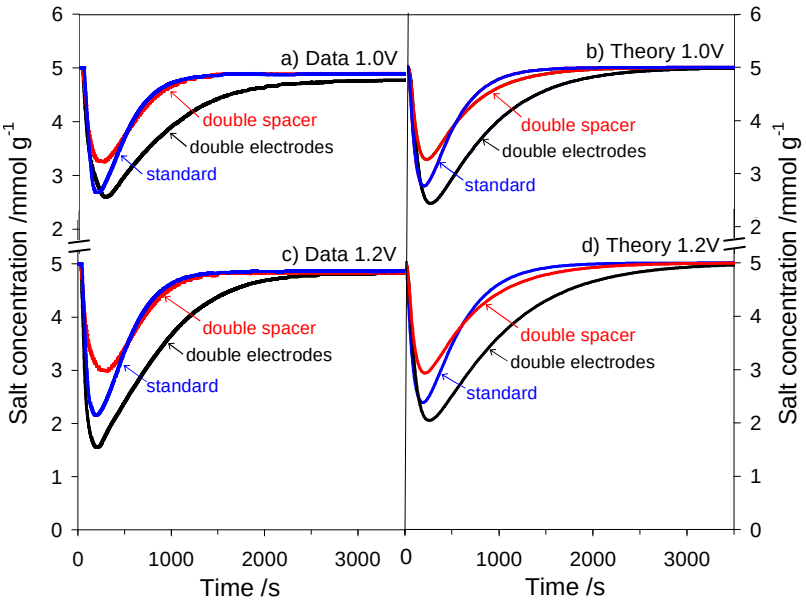

Fig. 6. Data (a,c) and theory (b,d) for effluent salt concentration as function of time and electrode thickness, spacer thickness and cell voltage, for a symmetric cell design.

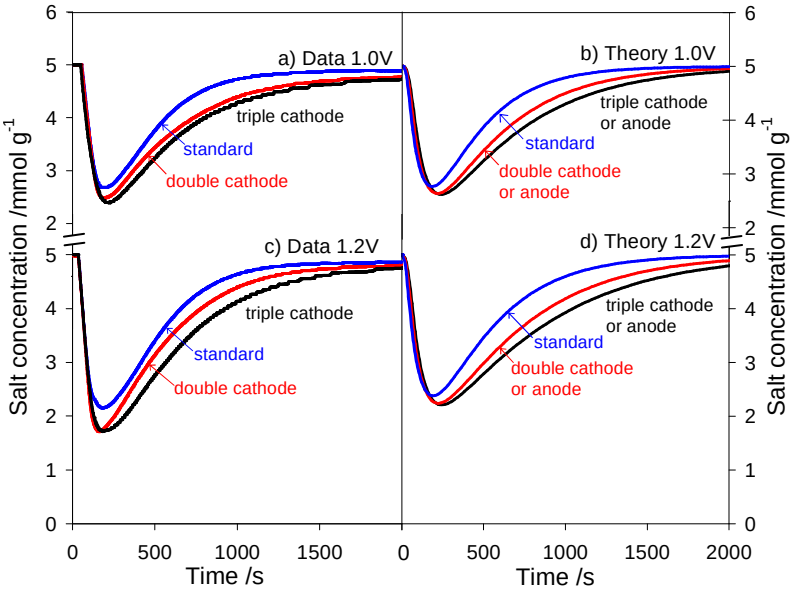

Fig. 7. Data (a,c) and theory (b,d) for effluent salt concentration as function of time and electrode thickness asymmetry, for V_{cell}=1.0 V (a,b) and 1.2 V (c,d).

In conclusion, various data sets have been presented for CDI experiments using several geometries; data both for equilibrium, and for the dynamic evolution of the effluent concentration. These data are well described by a simple model using a single set of parameter settings, a model based on using the cell voltage applied between the two electrodes as the key operational parameter. Because influent pH has no significant effect (if at all) on measured equilibrium properties, we can conclude that for the materials tested and under the chosen conditions, chemical surface charge effects do not seem to have an impact on the stored electronic charge, and neither on salt adsorption

in the EDLs. Therefore, in this case it seems not unreasonable to conclude that the EDL-structure in the micropores is basically independent of the sign of charge, and thus the assumption of similarity can be made. This implies that in a two-electrode design and with equal masses of electrodes, the applied cell voltage will be equally divided over the two electrodes. This may seem like a rather minor conclusion, but it has significant implications for how we understand the CDI technology, and for the choice of direction where to search for system improvements.

5. Conclusions

An extensive data set is presented for the performance of two-electrode flow cells used for water desalination (capacitive deionization, CDI), both for equilibrium (maximum) salt adsorption and for charge, as well as for the dynamic development of the effluent salt concentration. We present data for various values of salt concentration, cell voltage, pH of the feed solution, spacer channel thickness, and electrode thickness. The electrode thickness is varied in a symmetric fashion, by doubling the thickness of both electrodes, and in an asymmetric fashion by doubling and tripling the thickness (mass) of one electrode but not of the other. We extensively compare the situation of doubling and tripling the anode mass, with the reverse case where the cathode mass is increases twofold and threefold.

All of these observations are accurately described by theory that considers the cell voltage (voltage difference between the two electrodes) and the resulting charge transfer from one to the other electrode, as the primary factors determining the salt adsorption capacity and dynamics in the system tested. Especially the observation that system performance is unchanged when we go from double (triple) anode mass to the reverse situation (double or triple cathode mass) shows that the electrical double layer structure (EDL structure) is basically independent of the sign of the electronic charge. This must imply that for a cell with an equal amount of anode and cathode, and which is not (pre-)charged by external means in any way, the anode EDL has the same structure as the cathode EDL, except for the difference in sign. Our results were obtained for identical electrodes made of activated carbon powders that are not chemically modified to give them optimized anode or cathode functionality. We suggest that asymmetric testing as explained in this paper is an important tool to determine the effect of chemical modification of one or both electrodes.

We find no effect of feed pH on charge and salt adsorption, suggesting that the chemical surface charge present on the carbon has no, or only a minor, effect on salt adsorption and on electrode charge, at least for our experimental conditions and for our electrodes made of activated carbon particles which did not undergo dedicated chemical modifications to give them a permanent chemical charge.

The modified Donnan (mD) model has been extended to describe salt adsorption and charge in asymmetric systems, and describes data very well. The CDI transport model (which includes the mD model) has likewise been successfully applied for the various data sets.

Acknowledgements

This work was performed in the TTIW-cooperation framework of Wetsus, Centre of Excellence for Sustainable Water Technology. Wetsus is funded by the Dutch Ministry of Economic Affairs, the European Union Regional Development Fund, the Province of Friesland, the City of Leeuwarden, and the EZ/Kompas program of the ‘Samenwerkingsverband Noord-Nederland’. We thank the participants

of the themes “Capacitive Deionization” and “Advanced Waste Water Treatment” for their involvement in this research.

References

[1] A.A. Sonin, R.F. Probstein, Desalination, 5 (1968) 293.
[2] H. Strathmann, Ion-Exchange Membrane Separation Processes, Elsevier, Amsterdam, 2004.
[3] S.J. Kim, S.H. Ko, K.H. Kang, J. Han, Nature Nanotechnology, 5 (2010) 297.
[4] M. Pasta, C.D. Wessells, Y. Cui, F. La Mantia, Nano Letters, 12 (2012) 839.
[5] J.W. Blair, G.W. Murphy, Advances in Chemistry Series, 27 (1960) 206.
[6] B.B. Arnold, G.W. Murphy, Journal of Physical Chemistry, 65 (1961) 135.
[7] A.M. Johnson, J. Newman, Journal of The Electrochemical Society, 118 (1971) 510.
[8] Y. Oren, A. Soffer, Journal of Applied Electrochemistry, 13 (1983) 473.
[9] J.C. Farmer, D.V. Fix, G.V. Mack, R.W. Pekala, J.F. Poco, Journal of the Electrochemical Society, 143 (1996) 159.
[10] M.W. Ryoo, G. Seo, Water Research, 37 (2003) 1527.
[11] T.J. Welgemoed, C.F. Schutte, Desalination, 183 (2005) 327.
[12] K.-K. Park, J.-B. Lee, P.-Y. Park, S.-W. Yoon, J.-S. Moon, H.-M. Eum, C.-W. Lee, Desalination, 206 (2007) 86.
[13] Y. Oren, Desalination, 228 (2008) 10.
[14] L. Zou, L. Li, H. Song, G. Morris, Water Research, 42 (2008) 2340.
[15] P.M. Biesheuvel, Journal of Colloid and Interface Science, 332 (2009) 258.
[16] P.M. Biesheuvel, B. van Limpt, A. van der Wal, J. Phys. Chem. C, 113 (2009) 5636.
[17] K.C. Leonard, J.R. Genthe, J.L. Sanfilippo, W.A. Zeltner, M.A. Anderson, Electrochimica Acta, 54 (2009) 5286.
[18] L. Pan, X. Wang, Y. Gao, Y. Zhang, Y. Chen, Z. Sun, Desalination, 244 (2009) 139.
[19] H.B. Li, T. Lu, L.K. Pan, Y.P. Zhang, Z. Sun, Journal of Materials Chemistry, 19 (2009) 6773.
[20] M.A. Anderson, A.L. Cudero, J. Palma, Electrochimica Acta, 55 (2010) 3845.
[21] M. Wang, Z.-H. Huang, L. Wang, M.-X. Wang, F. Kang, H. Hou, New Journal of Chemistry, 34 (2010) 1843.
[22] R. Zhao, P.M. Biesheuvel, H. Miedema, H. Bruning, A. van der Wal, The Journal of Physical Chemistry Letters, 1 (2010) 205.
[23] J.-H. Lee, W.-S. Bae, J.-H. Choi, Desalination, 258 (2010) 159.
[24] S.-J. Seo, H. Jeon, J.K. Lee, G.-Y. Kim, D. Park, H. Nojima, J. Lee, S.-H. Moon, Water Research, 44 (2010) 2267.
[25] E. Avraham, M. Noked, Y. Bouhadana, A. Soffer, D. Aurbach, Electrochimica Acta, 56 (2010) 441.
[26] I. Cohen, E. Avraham, M. Noked, A. Soffer, D. Aurbach, J. Phys. Chem. C, 115 (2011) 19856.
[27] E. Avraham, M. Noked, I. Cohen, A. Soffer, D. Aurbach, Journal of the Electrochemical Society, 158 (2011) 168.
[28] T. Humplik, J. Lee, S.C. O'Hern, B.A. Fellman, M.A. Baig, S.F. Hassan, M.A. Atieh, F. Rahman, T. Laoui, R. Karnik, E.N. Wang, Nanotechnology, 22 (2011) 292001.
[29] S. Porada, L. Weinstein, R. Dash, A. van der Wal, M. Bryjak, Y. Gogotsi, P.M. Biesheuvel, ACS Applied Materials & Interfaces, 4 (2012) 1194.
[30] Z.-H. Huang, M. Wang, L. Wang, F. Kang, Langmuir, 28 (2012) 5079.
[31] J.-B. Lee, K.-K. Park, H.-M. Eum, C.-W. Lee, Desalination, 196 (2006) 125.
[32] H. Li, Y. Gao, L. Pan, Y. Zhang, Y. Chen, Z. Sun, Water Research, 42 (2008) 4923.
[33] P.M. Biesheuvel, A. van der Wal, Journal of Membrane Science, 346 (2009) 256.
[34] Y.-J. Kim, J.-H. Choi, Water Research, 44 (2010) 990.
[35] P.M. Biesheuvel, R. Zhao, S. Porada, A. van der Wal, Journal of Colloid and Interface Science, 361 (2011) 239.

[36] K.H. Mistry, R.K. McGovern, G.P. Thiel, E.K. Summers, S.M. Zubair, J.H. Lienhard V, Entropy, 13 (2011) 1829.
[37] B.B. Sales, M. Saakes, J.W. Post, C.J.N. Buisman, P.M. Biesheuvel, H.V.M. Hamelers, Environmental Science & Technology, 44 (2010) 5661.
[38] D. Brogioli, R. Zhao, P.M. Biesheuvel, Energy & Environmental Science, 4 (2011) 772.
[39] P.M. Biesheuvel, Y.Q. Fu, M.Z. Bazant, Physical Review E, 81 (2011) 031502.
[40] J.E.Z. Unda, E. Roduner, Physical Chemistry Chemical Physics, 14 (2012) 3816.
[41] D.J. Bonthuis, S. Gekle, R.R. Netz, Physical Review Letters, 107 (2011) 166102.
[42] S. Kondrat, V. Presser, C.R. Perez, Y. Gogotsi, A.A. Kornyshev, Energy & Environmental Science, 5 (2012) 6474.
[43] P.M. Biesheuvel, M.Z. Bazant, Physical Review E, 81 (2010) 031502.
[44] B. Kastening, M. Heins, Electrochimica Acta, 50 (2005) 2487.
[45] D.C. Grahame, Chemical Reviews, 41 (1947) 441.
[46] M.Z. Bazant, K.T. Chu, B.J. Bayly, SIAM Journal on Applied Mathematics, 65 (2005) 1463.

TOC picture